Preparation and Utilization of Catalyst-Functionalized Single-Walled Carbon Nanotubes for Ring-Opening Metathesis Polymerization

Yuanqin Liu and Alex Adronov*

Department of Chemistry and the Brockhouse Institute for Materials Research, McMaster University, Hamilton, Ontario L8S 4M1, Canada

Received December 19, 2003; Revised Manuscript Received April 28, 2004

ABSTRACT: Single-walled carbon nanotubes were oxidatively shortened and functionalized with ruthenium-based olefin metathesis catalysts. These catalyst-functionalized nanotubes were shown to be effective in the ring-opening metathesis polymerization of norbornene, resulting in rapid polymerization from the catalyst sites on the nanotube. It was found that high polymer molecular weights could be reached, and the molecular weight increased linearly with polymerization time. The resulting polynorbornene-functionalized nanotubes were found to exhibit solubility in organic solvents, whereas the starting materials and catalyst-functionalized nanotubes were completely insoluble. The polymerized materials were characterized by NMR, IR, DSC, AFM, and TEM.

Introduction

It is now well established that the unique structural and electronic properties of carbon nanotubes position them as one of the leading materials for a wide array of potential nanotechnological applications.[1,2] As part of the ongoing progress toward expanding their utility, the preparation of carbon nanotube derivatives, through chemical modification, has been the subject of intense recent interest.[3] One of the main goals of this work is the improvement of nanotube solubility in various organic and aqueous solvents, as well as their miscibility with bulk materials, such as polymers.[4] It has been identified that one of the most promising approaches to the realization of both of these goals is the covalent functionalization of carbon nanotubes with polymers.[5] The resulting materials would combine the high mechanical strength and electronic conductivity of carbon nanotubes with the solubility and processability of appended macromolecules, allowing them to be homogeneously dispersed in bulk polymers without the danger of phase separation. Such nanotube-loaded materials may become useful as conducting layers within a host of organic electronic devices, such as light-emitting diodes, photovoltaics, and thin-film transistors. A number of reports have demonstrated the feasibility of attaching amine- and alcohol-functionalized polymeric structures to the surface of single-walled carbon nanotubes (SWNTs) through amidation and esterification with the carboxylic acid moieties at the ends and defect sites of shortened SWNTs. Using this "grafting to" approach, SWNT conjugates with poly(ethylene imine),[6] poly(styrene),[7] poly(ethylene oxide),[8] poly(vinyl carbazole),[9] and poly(vinyl alcohol)[10] have been prepared. An alternative method that has recently been exploited by our group involves a "grafting from" approach that requires the attachment of polymerization initiators to the nanotubes followed by reaction with appropriate monomers.[11] Since this strategy involves the reaction of nanotubes with small molecules (initiators and monomers, rather than full-length polymers), loss of reactivity due to steric crowding on the nanotube surface is not an issue and should result in higher grafting density. Additionally, this approach benefits from its modular nature, where the preparation of a single initiator-functionalized nanotube sample can be used for the polymerization of a wide variety of monomers. We, and others,[12−14] have already shown that it is possible to polymerize various monomers using atom transfer radical polymerization (ATRP), resulting in nanotube structures for which the solubility is controlled by the nature of the attached polymers.

In an attempt to expand this general polymerization strategy, we have undertaken the investigation of nonradical approaches to polymer growth. One such approach is ring-opening metathesis polymerization (ROMP) using ruthenium alkylidene catalysts.[15] This polymerization method has attracted significant attention due to its versatility, effectiveness, and functional group tolerance, allowing for a variety of monomers bearing polar, apolar, and charged functional groups to be successfully polymerized.[16] It has recently been shown that extremely narrow polydispersities and excellent control over polymer molecular weight and architecture can be achieved if appropriate ligands are utilized, where high ligand dissociation rates result in rapid initiation of polymerization.[17,18] All of these factors have made ROMP a useful methodology for the functionalization of surfaces such as Si and SiO_2.[19,20] In fact, successful ROMP from the surface of SWNTs, where the ruthenium alkylidene catalysts were physisorbed on the nanotube surface using pyrene molecules as anchors has already been demonstrated.[21] Although this strategy resulted in successful polymerization and the production of polymer-coated SWNTs, it was shown that high molecular weight polymers tended to desorb from the nanotube surface, as evidenced by a decrease in the nanotube coating thickness when the polymerization time exceeded 5−10 min.[21]

As an alternative to this supramolecular polymer functionalization, we report here the covalent attachment of ROMP catalysts to the ends and defect sites of shortened SWNTs, and their subsequent utilization in the controlled polymerization of norbornene monomers.

* To whom correspondence should be addressed. Address: Department of Chemistry, McMaster University, 1280 Main St. W., Hamilton, Ontario L8S 4M1, Canada. Tel: (905) 525-9140 ext. 23514. Fax: (905) 521-2773. E-mail: adronov@mcmaster.ca.

10.1021/ma0359584 CCC: $27.50
Published on Web 06/02/2004

Scheme 1

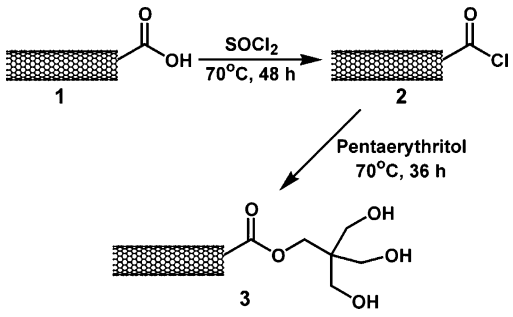

Scheme 2

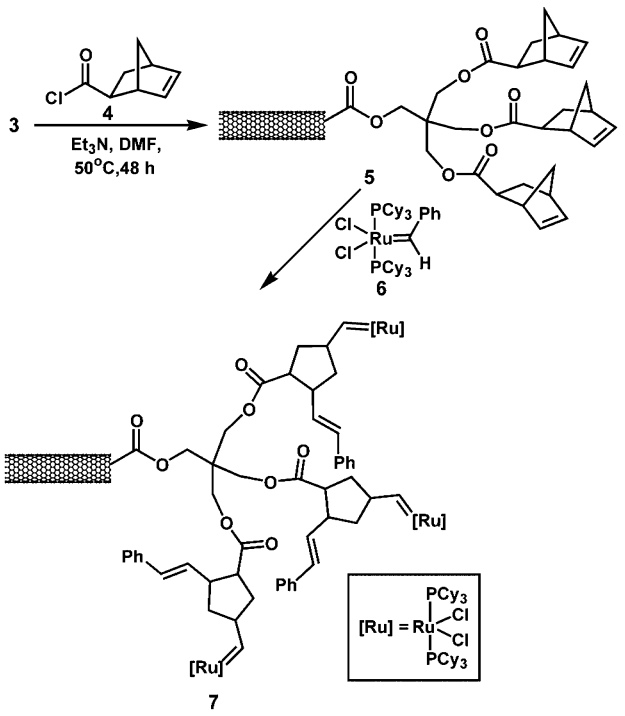

We demonstrate that it is possible to graft high molecular weight polymers to the nanotube surface, allowing for the modification of nanotube properties.

Results and Discussion

SWNTs, purchased from Carbon Nanotechnologies Inc., were initially shortened by sonication in H_2SO_4/HNO_3 for 2 h. This procedure resulted in carboxylic acid-functionalized nanotubes having lengths in the range of 330 nm.[11] The acid groups were converted to acid-chlorides using thionyl chloride (Scheme 1) and were then treated with pentaerythritol, resulting in the introduction of three primary alcohol functionalities for every reacted acid group of the nanotube. The triol-functionalized nanotubes (**3**) were then treated with the acid-chloride derivative of 5-norbornene-2-carboxylic acid (**4**) to produce the norbornene-functionalized nanotubes (**5**) which could subsequently be reacted with benzylidene-bis(tricyclohexylphosphine)dichloro-ruthenium (1st generation Grubbs catalyst, **6**), resulting in the formation of catalyst-functionalized nanotubes, **7** (Scheme 2). This product was isolated by filtration through a 200 nm-pore diameter Teflon membrane, followed by extensive washing with methanol, dichloromethane, and hexanes to remove any unreacted catalyst. The isolated nanotubes (**7**) can be considered as nanotube-based macroinitiators for ROMP. Due to the insolubility of the products formed in each of these synthetic steps, their characterization was limited to infrared (IR) spectroscopy. Figure 1 illustrates the IR spectra for the shortened, but unfunctionalized, SWNTs (A) as well as the norbornene-functionalized (B) and catalyst-functionalized (C) structures. The IR spectrum of the shortened nanotubes (Figure 1A) depicts the expected C═O stretch at 1748 cm^{-1} corresponding to the carboxylic acid groups introduced as a result (Scheme 2) of the shortening process. The large IR band observed at 3400 cm^{-1} and the weak one at 1632 cm^{-1} are attributed to the asymmetric bending and scissoring vibrations, respectively, due to trace amounts of water present in the KBr pellet used for the measurement.[11] In Figure 1B, the carbonyl stretch at 1737 cm^{-1} is clearly indicative of the ester bond formation between the norbornene and the alcohol of the SWNTs in compound **5**. In addition, the appearance of the C−H stretching frequencies at 2883 and 2968 cm^{-1} correspond to the added alkyl groups in the transformation from **1** to **5**. Spectroscopic evidence for the conversion of **5** to **7** is more subtle, but can be gathered from an increase in the intensity of the C═C stretch at 1660

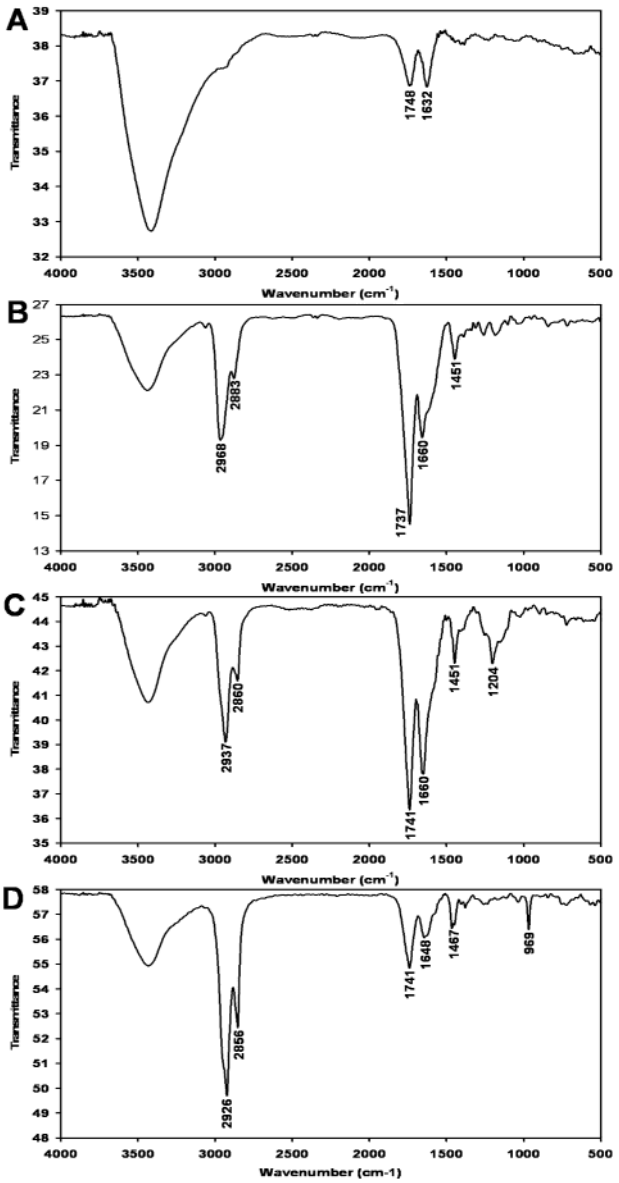

Figure 1. IR spectra of compounds **1** (A), **5** (B), **7** (C), and **8** (D).

Scheme 3

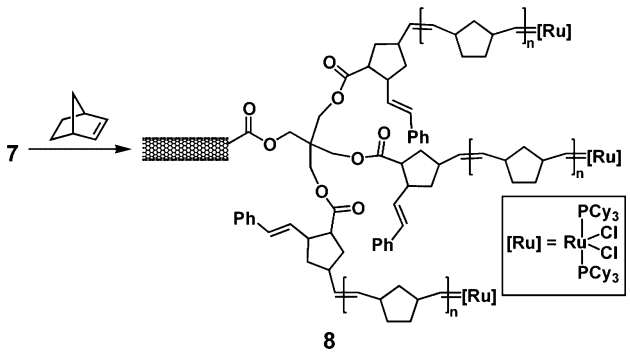

cm^{-1} relative to the carbonyl stretch at 1741 cm^{-1}. However, the definitive evidence for the preparation of the SWNT macroinitiator **7** was derived from its ability to promote ROMP. Addition of norbornene to a suspension of **7** in degassed chloroform or heptane resulted in a rapid polymerization from the surface of the nanotubes (Scheme 3). Typical polymerization times ranged from 5 to 180 min. The polymerization products were isolated by filtration through a 200 nm pore-diameter Teflon membrane, followed by thorough washing with dichloromethane, THF, and methanol. The IR spectrum of a typical polymerized product (2 h polymerization time) is depicted in Figure 1D. The significant intensity of the C−H stretches at 2856 and 2926 cm^{-1} is indicative of the increased number of alkyl groups within the product as a result of norbornene polymerization and is consistent with the IR of polynorbornene itself. It should be noted that any free polymer that may be formed in solution is easily removed by the filtration/washing step of the workup. Control experiments, where the polymerization was carried out in the presence of SWNTs, but with unattached catalyst **6**, resulted in no detectable attachment of polymers to the nanotubes, as evidenced by the absence of any change in the IR spectrum of the isolated nanotube product from that of the starting material.

Figure 2 illustrates the Raman spectra of the shortened, unfunctionalized nanotubes and the polymerized nanotubes (**8**). In both cases, the characteristic absorptions of the nanotubes are clearly observable at ca. 260 and 1590 cm^{-1}, corresponding to the radial breathing modes (RBM) and the tangential G band, respectively.[22] In addition, the broad disorder band at 1300 cm^{-1} indicates the presence of sp^3 hybridized C atoms, which are known to occur at defect sites in the nanotube structure.[23] The strong similarity between the two Raman spectra indicates that the functionalization and polymerization processes did not significantly alter the nanotube structure.

It was found that the solubility of the polymerized nanotubes was influenced by the appended polymers. Prior to the polymerization step, the catalyst-functionalized nanotubes were completely insoluble in all organic solvents. However, after polymerization, the nanotubes became slightly soluble in THF, chloroform, and dichloromethane (Figure 3). Utilizing the previously published specific extinction coefficient for SWNTs (ϵ_{500} = 28.6 cm^2/mg),[24] we were able to estimate the nanotube concentration to be ca. 19 mg/L. Although quite low, this level of solubility nevertheless allowed for the use of solution NMR in the characterization of the polymerized structures. Figure 4 depicts the ^1H NMR spectra of polynorbornene and the polymerized nanotubes **8**. The

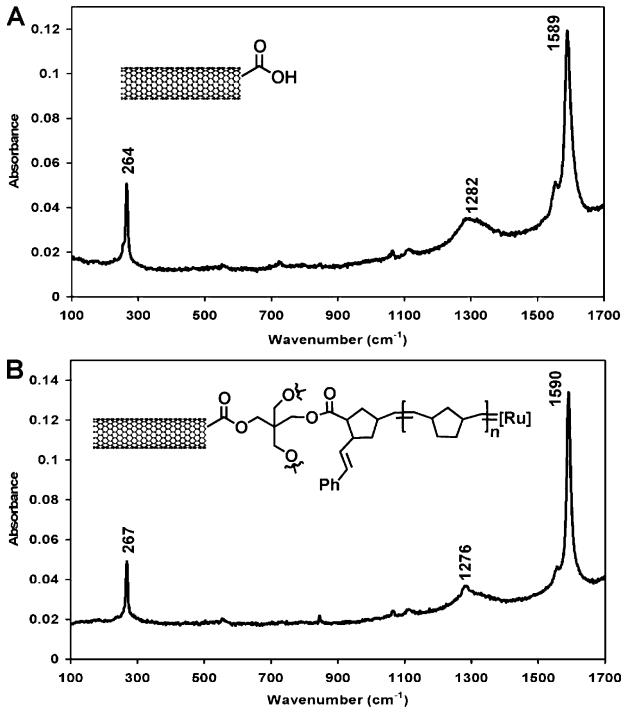

Figure 2. Raman spectra of shortened nanotubes (A) and polynorbornene-functionalized nanotubes (B).

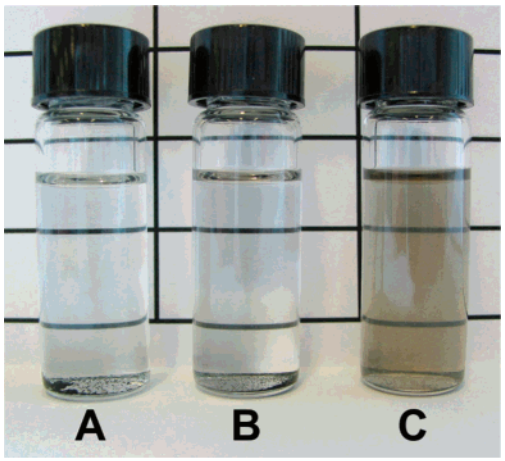

Figure 3. Samples of shortened, unfunctionalized nanotubes **1** (A), Grubbs catalyst-functionalized nanotubes **7** (B), and polymerized nanotubes **8** (C) in THF.

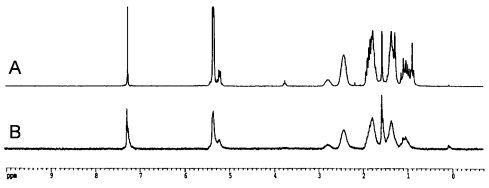

Figure 4. ^1H NMR spectra of polynorbornene (A) and polynorbornene-functionalized nanotubes (B).

two spectra are nearly identical, indicating that norbornene monomers were, indeed, polymerized with the use of the nanotube macroinitiators.

To further explore the topological properties of the hybrid materials, we utilized atomic force microscopy (AFM). Sample preparation involved spin-coating several drops of the nanotube solution onto a mica substrate. Prior to polymerization, the initiator-functionalized nanotubes were indistinguishable from typical unfunctionalized structures, associating in small bundles

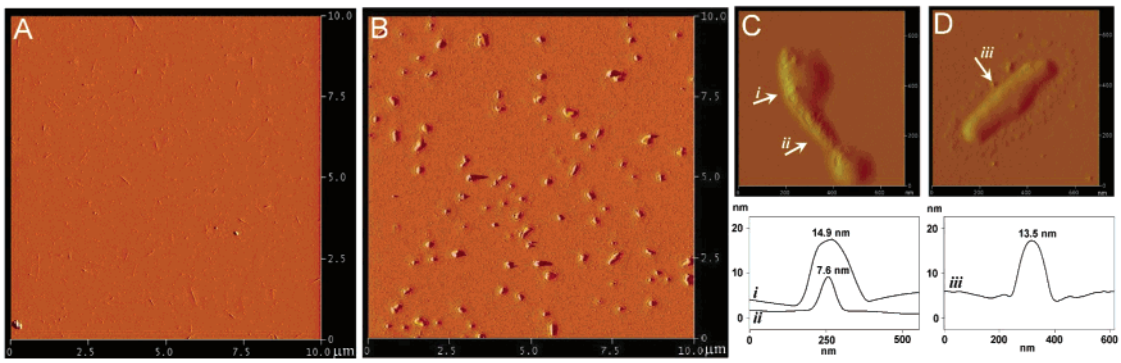

Figure 5. AFM images of nanotubes before (A) and after (B) polymerization. Two close-ups of individual structures, (C) and (D), illustrate that the polymer density can be localized near the ends of the tubes in some cases (C) and along the entire wall of the tubes in others (D). Profile traces at different points along the features are given below the AFM images (C) and (D).

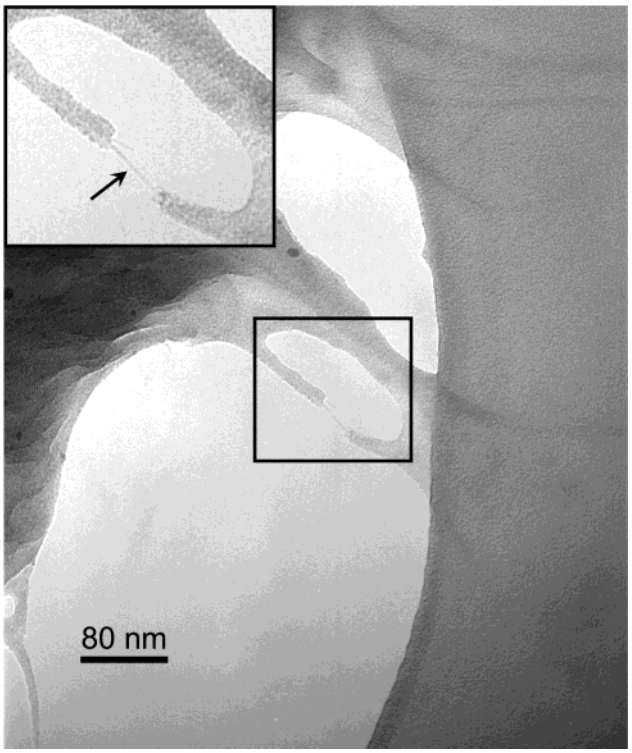

Figure 6. TEM image of polymerized nanotubes. The inset is a blow-up of the region within the box, showing a single nanotube bridging the gap between two polymer regions (arrow).

with diameters in the range of 1−3.5 nm (Figure 5A). However, after polymerization, larger features were observable, corresponding to SWNTs that are surrounded by domains of polymer (Figure 5B). In some cases, it was possible to observe larger polymer domains near the ends of the nanotubes, likely because most of the initiators were attached to the carboxylic acid groups mainly located at the open nanotube ends (Figure 5C). Other structures seemed to have polymer regions evenly distributed along the entire length of the nanotube, likely due to polymer wrapping or the attachment of polymerization catalysts at defect sites along the side walls of the nanotubes (Figure 5D). Height profiles for the polymerized structures indicated that the height of the features increased to 8−15 nm as a result of the appended polymer structures (see the profile traces below images C and D of Figure 5). However, it is not possible to ascertain whether the observed features contain individual nanotubes or bundles of tubes.

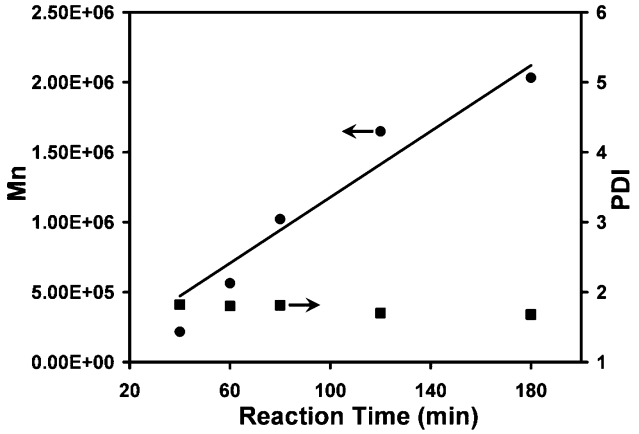

Figure 7. Plot of the molecular weight and polydispersity of polynorbornene cleaved from the SWNTs as a function of polymerization time.

Further characterization of the polymerized nanotubes was done using transmission electron microscopy (TEM), as depicted in Figure 6. Again, solutions of **8** in THF were drop-cast onto a holey carbon-coated copper grid and allowed to air-dry. Low magnification TEM images highlighted the presence of sheets and fibers of amorphous carbon in which, upon close inspection, it was possible to discern the presence of SWNTs. It appeared as though the nanotubes were embedded within a matrix of amorphous carbon, which corresponds to the polymer coating on the SWNTs. In some areas, it was also possible to observe portions of single nanotubes spanning the gap between two regions of polymer (Figure 6, inset).

To determine the effect of polymerization time on polymer molecular weight, we analyzed the polymers produced in a series of polymerizations that ranged from 5 to 180 min in duration. Nanotube bound polymers were cleaved by saponification of the ester linkages with KOH/18-crown-6 in THF for 48 h at room temperature. The SWNTs were separated from the cleaved polymer by filtration through a 200 nm pore-diameter membrane, leaving the pure polymer in the filtrate. SEC analysis of the isolated polymers revealed a linear increase in molecular weight with increasing polymerization time (Figure 7). The polydispersities of the samples were found to remain relatively constant at all polymerization times.

It was also possible to measure the glass transition temperature of the polynorbornene before and after cleavage from the nanotubes. The nanotube bound

polymers were found to exhibit a T_g of 37 °C. After cleavage, the T_g was found to decrease to 27 °C, which is very similar to previously reported literature values for polynorbornene.[25] The higher T_g observed for the nanotube-bound polymers is due to their decreased mobility as a result of nanotube attachment and is consistent with our earlier observations with PMMA-functionalized nanotubes,[11] as well as other literature reports of surface-bound polymers.[26]

Conclusions

We have demonstrated that it is possible to functionalize shortened SWNTs with ruthenium alkylidene catalysts by utilizing the acid groups formed at the ends and defect sites of nanotubes as a result of the shortening process. The catalyst-functionalized nanotubes are effective initiators of norbornene polymerization. The polymerizations were shown to result in the formation of polynorbornene-functionalized nanotubes, which had a slightly improved solubility in organic solvents. The polymer molecular weights were shown to increase linearly with time, and the polydispersities were found to be consistent with expected values for the catalysts used. Future work will involve the attachment of "third-generation" ruthenium-based olefin metathesis catalysts[17] that will result in narrower polydispersities, and will allow for the preparation of block copolymers. Sidewall functionalization of SWNTs with ROMP catalysts will also be investigated.

Experimental Section

General. Single-walled carbon nanotubes (SWNTs) were purchased from Carbon Nanotechnologies, Inc. (Houston, TX). *N*-(4-Hydroxyphenyl)glycine was purchased from Aldrich and purified by recrystallization in distilled H_2O. Pentaerythritol, octyl aldehyde, 5-norbornene-2-carboxylic acid, acryloyl chloride, thionyl chloride, 18-crown-6, triethylamine, benzylidene-bis(tricyclohexylphosphine)dichlororuthenium (Grubbs catalyst, 1st generation), and norbornene were all purchased from Aldrich and used without further purification. All other reagents and solvents were purchased from commercial suppliers and used as received. FTIR was performed on a Bio-Rad FTS-40 instrument. All samples were prepared as pellets using spectroscopic grade KBr in a Carver press at 15 000 psi. Laser Raman spectroscopy was performed on a Bruker RFS 100 instrument equipped with a YAG laser and a Ge high-sensitivity detector. AFM was done using a Digital Instruments NanoScope IIIa Multimode AFM, with samples prepared by spin casting (4000 rpm) sample solutions or suspensions on freshly cleaved mica substrates. The images were recorded with standard tips in tapping mode at a scan rate of 0.5 Hz. TEM analysis was performed using a Philips CM12 operating at 120 keV. NMR was performed on a Bruker 200 MHz instrument in $CDCl_3$. Differential scanning calorimetry (DSC) was performed on a TA 2100 Modulated Differential Scanning Calorimeter with a temperature gradient of 15°/min. Ultrasonication was done in a Banson Ultrasonics B1510 bath sonicator. Filtration was done through either a 100-nm pore diameter polycarbonate membrane (Millipore), or a 200-nm pore diameter Teflon membrane (Millipore). Polymer molecular weight and polydispersity index (PDI) were estimated by gel permeation chromatography (GPC) using a Waters 2695 Separations Module equipped with a Waters 2996 Photodiode Array Detector, a Waters 2414 Refractive Index Detector, a Waters 2475 Multi λ Fluorescence Detector, and four Polymer Labs PLgel individual pore size columns. Polystyrene standards were used for calibration, and tetrahydrofuran (THF) was used as the eluent at a flow rate of 1.0 mL/min. The concentrations of the soluble polymer functionalized SWNTs were calculated from UV/vis absorption results obtained using a Varian Cary 50 Bio UV−visible spectrophotometer.

Shortening and Purification of SWNTs. A 250 mL flask charged with SWNTs (100 mg) and a H_2SO_4/HNO_3 (v/v: 3/1) (120 mL) solution was sonicated for 2 h. Then the suspension was diluted in a 1000 mL beaker with distilled water (800 mL). After cooling to room temperature, the dilute solution was filtered through a 100-nm pore diameter polycarbonate membrane. The black material collected on the membrane was added to a 250 mL flask and stirred with H_2SO_4/H_2O_2 (v/v: 9/1, 50 mL) for 30 min at room temperature. Another 50 mL of H_2SO_4/H_2O_2 (v/v: 9/1) was added and the suspension was sonicated for 5 min. After dilution using distilled water (800 mL) in a 1000 mL beaker, the suspension was filtered again. The SWNT mat was washed thoroughly using NaOH solution (10 mmol, 250 mL) and distilled water until the pH of the filtrate was 7. Then the nanotubes were washed with an HCl solution (2.0 M, 50 mL) before drying under vacuum overnight. The product was obtained as a black solid (70.0 mg, 70% yield). IR (KBr pellet): ν = 1748 (m), 1632 (m).

Synthesis of Triol-Functionalized SWNTs (3). Shortened and purified SWNTs (44.0 mg) were added to thionyl chloride (10.0 mL, 137 mmol) in a 25 mL flame dried flask. The suspension was stirred under Ar at 70 °C for 48 h to convert the acid groups to acid chlorides. The residual thionyl chloride was evaporated in vacuo. Pentaerythritol (0.5 g, 3.7 mmol) and THF (10 mL) were then added into the flask. The suspension was stirred at 70 °C for another 36 h. The reaction mixture was then filtered through a 200-nm pore diameter Teflon membrane, followed by washing with CH_2Cl_2 (300 mL), THF (100 mL), and methanol (100 mL). The recovered residue was finally dried under vacuum overnight, yielding 50 mg of product. IR (KBr pellet): ν = 3442 (s), 2929 (w), 2871 (w), 1752 (w), 1656 (m).

Synthesis of Norbornene-Functionalized SWNTs (5). The mixture of 5-norbornene-2-carboxylic acid (3.0 mL, 24.5 mmol) and thionyl chloride (8 mL, 109.7 mmol, 4.5 eq.) in a flame-dried 25 mL flask was stirred at reflux under Ar for 24 h. It was then cooled, evaporated to dryness, and used directly. Triol-functionalized SWNTs (3) (48 mg) were added to the 5-norbornene-2-carboxylic acid chloride along with 10 mL of CH_2Cl_2, 1 mL of anhydrous DMF, and 1 mL of triethylamine. The suspension was stirred at 50 °C under Ar for 48 h. The product was isolated by filtration through a 200 nm-pore diameter Teflon membrane, followed by washing with methanol (300 mL), THF (100 mL), and CH_2Cl_2 (200 mL). The recovered residue was then dried under vacuum overnight, yielding 53 mg of product. IR (KBr pellet): ν = 2968 (m), 2883 (w), 1737 (s), 1660−1530 (br, m), 1451 (w).

Synthesis of Catalyst-Functionalized SWNTs (7). The norbornene-functionalized SWNTs (**5**) (51 mg), benzylidene-bis(tricyclohexylphosphine)dichlororuthenium catalyst (**6**) (20.0 mg, 2.4×10^{-2} mmol), and heptane (10.0 mL) were added into a 25 mL flask. The suspension was sonicated for 5 min and then stirred at room temperature for 12 h. The product was isolated by filtration through a 200-nm pore diameter Teflon membrane, followed by washing with methanol (200 mL), CH_2Cl_2 (200 mL), and hexanes (200 mL). The recovered residue was then dried under vacuum overnight. The resulting SWNT macroinitiator was isolated as a black powder (54 mg). IR (KBr pellet): ν = 2937 (s), 2860 (m), 1741 (m), 1660 (w), 1451 (w), 1204 (w).

General Procedure for Ring-Opening Metathesis Polymerization using the SWNT Macroinitiator. Approximately 3.0 mg of the SWNT macroinitiator (**7**) was dispersed in 10 mL of $CHCl_3$ by sonication for 5 min. The suspension was degassed by bubbling with nitrogen for 5 min, and a solution of norbornene (0.5 g, 5.3×10^{-3} mol) in 5 mL of $CHCl_3$ was added. The suspension was then stirred at room temperature for 5−180 min. The product was filtered through a 200 nm-pore diameter Teflon membrane, and washed with CH_2Cl_2 (300 mL), THF (300 mL), and methanol (100 mL). The recovered residue was then dried under vacuum overnight. IR (KBr pellet): ν = 2926 (s), 2856 (m), 1741 (m), 1648 (w), 1467 (w), 969 (w). ^{1}H NMR (200 MHz, $CDCl_3$): δ 0.91−1.19 (br), 1.19−1.48 (br), 1.64−1.97 (br), 2.20−2.55 (br), 2.70−2.90 (br), 5.12−5.40 (m).

General Procedure for Cleavage of Polynorbornene from the Polymerized SWNTs. A sample of the polynorbornene-functionalized SWNTs (8) (51.0 mg) was suspended in THF (50.0 mL) followed by the addition of ground KOH (0.2 g, 3.6 mmol) and 18-crown-6 (1.0 g, 3.8 mmol). The solution was then stirred at room temperature for 48 h. The reaction mixture was filtered through a 200-nm pore diameter Teflon membrane, followed by washing with THF (250 mL). This resulted in a black residue, composed of SWNTs, remaining on the membrane, with the filtrate containing the cleaved polynorbornene. The filtrate was concentrated to approximately 2 mL and precipitated into hexanes (100 mL). The precipitate was then filtered and dried under vacuum overnight, allowing the recovery of the cleaved polynorbornene as a white solid (20 mg). IR (KBr pellet): ν = 2956−2837 (br, m), 1660−1567 (br, m), 1470−1420 (br, m), 1351 (m), 1281 (w), 1250 (w), 1109 (s), 967 (m), 840 (w). ^{1}H NMR (200 MHz, $CDCl_3$): δ 0.91−1.19 (br), 1.19−1.48 (br), 1.64−1.97 (br), 2.20−2.55 (br), 2.70−2.90 (br), 5.12−5.40 (m).

Acknowledgment. This work was supported by grants from the Natural Science and Engineering Research Council of Canada (NSERC), the Canada Foundation for Innovation, the Ontario Innovation Trust, as well as McMaster University. Support in the form of a Premier's Research Excellence Award is also gratefully acknowledged. Additionally, we thank Mr. Bernard Pointner for the Raman spectroscopy data.

References and Notes

(1) Collins, P. G.; Avouris, P. *Sci. Am.* **2000**, *283*, 62−69.
(2) Dai, H. J. *Surf. Sci.* **2002**, *500*, 218−241.
(3) Hirsch, A. *Angew. Chem., Int. Ed.* **2002**, *41*, 1853−1859.
(4) Bahr, J. L.; Tour, J. M. *J. Mater. Chem.* **2002**, *12*, 1952−1958.
(5) Sun, Y. P.; Fu, K. F.; Lin, Y.; Huang, W. J. *Acc. Chem. Res.* **2002**, *35*, 1096−1104.
(6) Riggs, J. E.; Guo, Z. X.; Carroll, D. L.; Sun, Y. P. *J. Am. Chem. Soc.* **2000**, *122*, 5879−5880.
(7) Hill, D. E.; Lin, Y.; Rao, A. M.; Allard, L. F.; Sun, Y. P. *Macromolecules* **2002**, *35*, 9466−9471.
(8) Sano, M.; Kamino, A.; Okamura, J.; Shinkai, S. *Langmuir* **2001**, *17*, 5125−5128.
(9) Wu, W.; Zhang, S.; Li, Y.; Li, J. X.; Liu, L. Q.; Qin, Y. J.; Guo, Z. X.; Dai, L. M.; Ye, C.; Zhu, D. B. *Macromolecules* **2003**, *36*, 6286−6288.
(10) Lin, Y.; Zhou, B.; Fernando, K. A. S.; Liu, P.; Allard, L. F.; Sun, Y. P. *Macromolecules* **2003**, *36*, 7199−7204.
(11) Yao, Z.; Braidy, N.; Botton, G. A.; Adronov, A. *J. Am. Chem. Soc.* **2003**, *125*, 16015−16024.
(12) Qin, S. H.; Oin, D. Q.; Ford, W. T.; Resasco, D. E.; Herrera, J. E. *J. Am. Chem. Soc.* **2004**, *126*, 170−176.
(13) Kong, H.; Gao, C.; Yan, D. Y. *J. Am. Chem. Soc.* **2004**, *126*, 412−413.
(14) Baskaran, D.; Mays, J. W.; Bratcher, M. S. *Angew. Chem., Int. Ed.* **2004**, *43*, 2138−2142.
(15) Nguyen, S. T.; Johnson, L. K.; Grubbs, R. H. *J. Am. Chem. Soc.* **1992**, *114*, 3974−3975.
(16) Louie, J.; Grubbs, R. H. *Organometallics* **2002**, *21*, 2153−2164.
(17) Love, J. A.; Morgan, J. P.; Trnka, T. M.; Grubbs, R. H. *Angew. Chem., Int. Ed.* **2002**, *41*, 4035−4037.
(18) Choi, T. L.; Grubbs, R. H. *Angew. Chem., Int. Ed.* **2003**, *42*, 1743−1746.
(19) Juang, A.; Scherman, O. A.; Grubbs, R. H.; Lewis, N. S. *Langmuir* **2001**, *17*, 1321−1323.
(20) Kim, N. Y.; Jeon, N. L.; Choi, I. S.; Takami, S.; Harada, Y.; Finnie, K. R.; Girolami, G. S.; Nuzzo, R. G.; Whitesides, G. M.; Laibinis, P. E. *Macromolecules* **2000**, *33*, 2793−2795.
(21) Gomez, F. J.; Chen, R. J.; Wang, D. W.; Waymouth, R. M.; Dai, H. J. *Chem. Commun.* **2003**, 190−191.
(22) Rao, A. M.; Richter, E.; Bandow, S.; Chase, B.; Eklund, P. C.; Williams, K. A.; Fang, S.; Subbaswamy, K. R.; Menon, M.; Thess, A.; Smalley, R. E.; Dresselhaus, G.; Dresselhaus, M. S. *Science* **1997**, *275*, 187−191.
(23) Bahr, J. L.; Yang, J. P.; Kosynkin, D. V.; Bronikowski, M. J.; Smalley, R. E.; Tour, J. M. *J. Am. Chem. Soc.* **2001**, *123*, 6536−6542.
(24) Bahr, J. L.; Mickelson, E. T.; Bronikowski, M. J.; Smalley, R. E.; Tour, J. M. *Chem. Commun.* **2001**, 193−194.
(25) Finkelshtein, E. S.; Makovetskii, K. L.; Yampol'skii, Y. P.; Portnykh, E. B.; Ostrovskaya, I. Y.; Kaliuzhnyi, N. E.; Pritula, N. A.; Gol'berg, A. I.; Yatsenko, M. S.; Platé, N. A. *Makromol. Chem.* **1991**, *192*, 1−9.
(26) Savin, D. A.; Pyun, J.; Patterson, G. D.; Kowalewski, T.; Matyjaszewski, K. *J. Polym. Sci., Part B: Polym. Phys.* **2002**, *40*, 2667−2676.

MA0359584